NASA Technical Memorandum 104553

Assessment of Probability of Detection of Delaminations in Fiber-Reinforced Composites

E. J. Chern, H. P. Chu, and J. N. Yang

December 1991

NASA

NASA Technical Memorandum 104553

Assessment of Probability of Detection of Delaminations in Fiber-Reinforced Composites

E. J. Chern
H. P. Chu
Goddard Space Flight Center
Greenbelt, Maryland

J. N. Yang
Department of Civil Engineering
University of California, Irvine
Irvine, California

Table of Contents

I.   INTRODUCTION

Fiber-reinforced composites are attractive aerospace materials for their improved strength-to-weight ratio, wear and corrosion resistance, thermal and acoustical insulation, fatigue life, and other desirable properties. Unlike metallic materials, composites are generally inhomogeneous, anisotropic, and multilayered. Thus, the fracture mechanisms of composites are much more complex to model and predict. Especially for space applications, the material property and performance requirements are considerably more stringent compared to other non-space usages. However, a damage-tolerant designed composite structure can be attained by quantitative nondestructive evaluation (NDE) techniques on preexisting flaws. For this approach, it is essential to determine detection limits and probability of detection (POD)[1-2] of selected NDE techniques to ensure proper detection of critical defects.

Ultrasonic techniques[3-4] are the most commonly used NDE methods for detecting and characterizing defects in conventional materials, such as metals, and advanced materials, such as fiber-reinforced composites. Numerous research efforts have been conducted concerning various technical approaches for the detection of defects in composites. Delamination is one of the critical defects in composite materials and structures. The ultrasonic C-scan imaging technique[5-9], which maps out the acoustic impedance mismatched areas with respect to the sample coordinates, is particularly well suited for detecting and characterizing delaminations in composites. However, to properly interpret the ultrasonic C-scan results, it is necessary to correlate the indications with the detection limits and POD of the ultrasonic C-scan imaging technique.

For example, NASA Far Ultraviolet Spectroscopic Explorer (FUSE), Earth Observing System (EOS), and other space flight projects use composites as structural members for the spacecraft and instrument platforms. The baseline information on the assessment of POD of delaminations in composite materials and structures is very beneficial to the evaluation of spacecraft materials according to inspection requirements and fracture control plans for these projects. In this study, we review the background and principle of POD, describe the laboratory setup and test procedure, and present the results of the experiments, as well as assessment of POD of delaminations in fiber-reinforced composite panels using ultrasonic C-scan techniques.

II.   GENERAL BACKGROUND ON POD

The POD for a given NDE process involves three factors:
(a)   System parameters: instrumentation, probes, calibration, sensitivity, inspection procedure, operator, etc.
(b)   Material parameters: microstructure, surface finish, etc.
(c)   Defect parameters: location, orientation, type, size, shape, composition, etc.

For example, in ultrasonic C-scan inspection of a flat composite panel, the use of a pulser/receiver with specific setup parameters, a transducer of a given diameter and frequency, calibration sensitivity, mechanical scanning parameters, a designated inspector, and the inspection of certain defects, etc., must be considered in this specific NDE technique. The POD for a particular inspection process is defined when the inspection system, material, and defect parameters are specified.

POD can be used in two ways. One is to determine the detection limits of a specific NDE technique for a specific type of defect in a material and structure. The other is to optimize the inspection parameters of the system for the effective and efficient NDE inspection. A typical mean POD curve of an inspection process is shown in Figure 1. The mean POD is about 90%; i.e., on average, 90% of defects of a considered size will be detected. Note that this is not the same as stating that an individual defect of that size will be detected 90% of the time it is inspected. A specific defect may have higher or lower POD than the mean value, depending on its characteristics. The monotonic increase in POD with increasing flaw size is found for almost all inspection techniques and corresponds well with physical reality.

Ideally, in order to determine POD, we should measure what proportion of flaws is actually detected from the potentially infinite population of flaws of a given type. In reality, at best, we can expect to have available only a relatively small sample of these flaws to represent the population and the distribution of defects for POD study. Statistical analysis can then be applied to the data base obtained from an inspection of the defect sample to estimate the true capability of the NDE technique. Two sources generally are used to create the desired sampling base: (a) Detected natural defects - this requires collection of defective hardware. However, in most
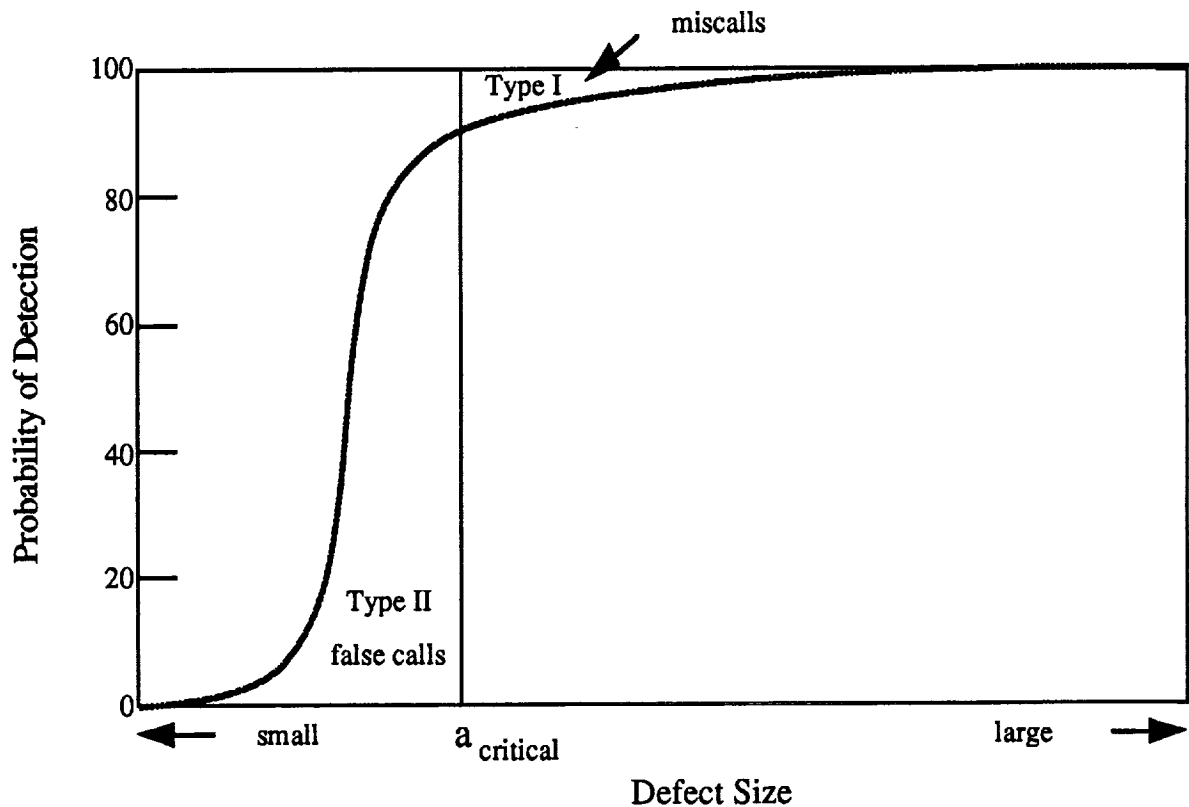
2

Figure 1. Typical POD Curve of an NDE Inspection

cases, a limited number of flaws exists, but the actual hardware is very costly; (b) Simulated defect specimens - simulated defects are generated on smaller specimens, having a wide range of flaw parameters considered to be a close representation of the actual distribution in the natural population.

In both approaches, a referee technique of higher fundamental sensitivity than the inspection technique being evaluated must be found. Because the sampling base for determining POD should consist of both detectable and undetectable defects for the NDE technique used. The use of a more sensitive inspection method is necessary to detect and establish the existence of the defects not found by the inspection process. For example, a high-power optical microscope is frequently used as a referee technique for surface flaws. In some cases, both nondestructive and destructive evaluations will be necessary to establish the total sample characteristics.

Since the determination of POD is based on results of inspection on the sampling defect base, it is crucial that the sampling base adequately represents the true distribution and population of defects, as well as satisfies the statistical analysis requirements. An example of a probability distribution of a defect population is shown in Figure 2. The typical defect distribution is Gaussian.

There are many parameters associated with any given type of defect. Thus, more than one distribution of characteristics is likely to be involved. For example, for delaminations in composites, there will be distribution of a range of delamination sizes, and for each size, a distribution of delamination shapes, depths, and locations. However, usually only the more obvious parameter can be adequately represented in selecting a sampling base. The influence of other defect parameters, together with the effects of the selected inspection process, will become apparent in the differences in detectability exhibited by various flaws of equal size.

Statistical requirements concern both the total number of samples and their distribution. In general, a sample size of at least 40-50 flaws is desirable in order to produce a reasonably smooth pattern or behavior for the POD curve, and to provide a reasonably
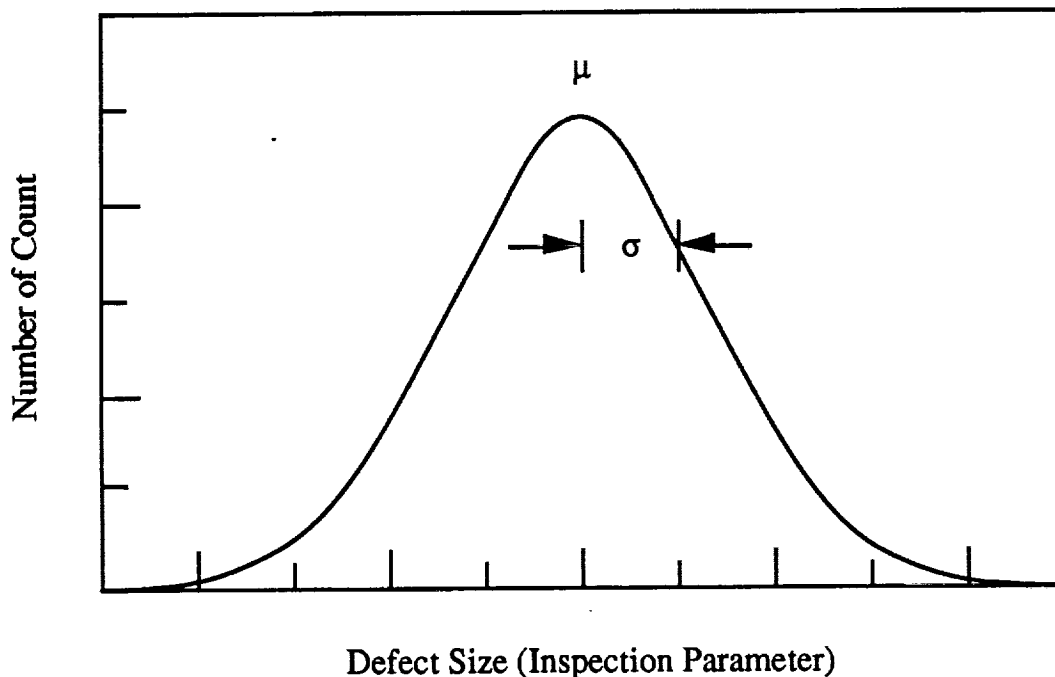

Figure 2. An Example of Defect Distribution

narrow confidence band for the calculated POD estimates. It is also desirable to ensure that the sample contains flaws of sizes that are below, roughly equal to, and above the 50% mean POD size. We also should consider the flaws to represent a random sample of the population, from a statistical point of view.

Furthermore, we implicitly assume that the population is well-behaved in terms of conformance to a standard distribution. We may then use the behavior of the sample to predict the behavior of the population. Thus we equate the proportion of flaws detected in the sample to the best estimate of the mean POD for the population. However, we acknowledge that from a similar but nonidentical sample we should expect to get a slightly different answer. The statistical approach allows us to estimate how confident we are that any individual best estimate correctly represents the population.

After all the samples are inspected, the chosen statistical method is applied to analyze the data and determine the POD. Typically, either binomial distribution statistics or a regression method is used. Much effort is being devoted to developing new and improved statistical procedures to provide the closest approximation of the "true" POD with the minimum number of samples.

For a given NDE inspection procedure, the detection limit, a_{NDE}, is generally defined by a high detection probability and a high confidence level. This is used for life management purposes since it provides a single defect size estimate that can be used in fracture mechanics calculations as the initial defect size. The ideal POD curve is a unit step function at the critical defect size, as shown in Figure 3, which means that the NDE technique used will detect all the defects equal to or greater than the critical defect size and will not detect defects smaller than the critical defect size.

Generally, for any NDE inspection relative to a desired detection threshold such as a_{NDE}, there will be two types of error associated with the inspection process: (a) Type I error: failure to give a positive indication when the defect size is greater than a_{NDE}, i.e., missed calls; and (b) Type II error: giving a positive indication when the defect size is smaller than a_{NDE}, i.e., false calls. For safety reasons, Type I errors, missed calls, are of primary concern. However, for program cost management, Type II errors, false calls, are equally important. Type I and Type II errors are inherent to an inspection process and can only be improved with redundant inspections.
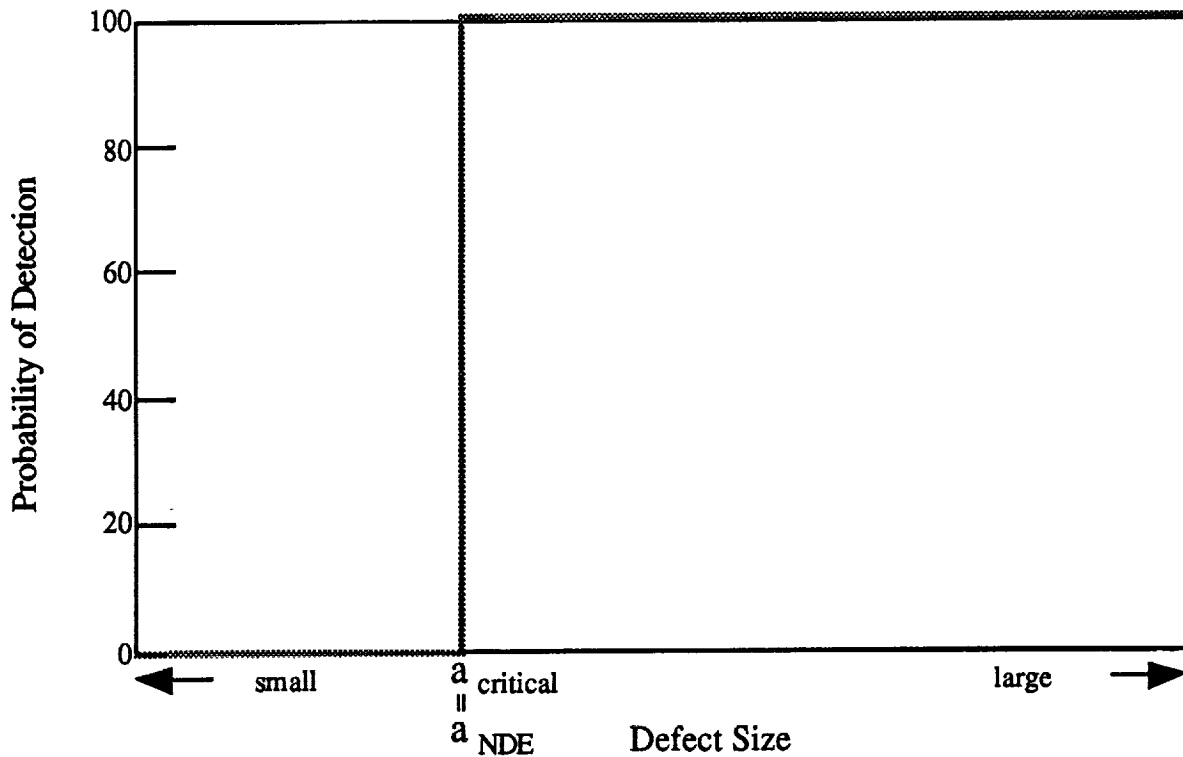
5

Figure 3. Ideal POD Curve of an NDE Inspection

We should note that once the NDE technique and test procedure have been established, even though the specific POD curve has not necessarily been determined, the POD inherent in this particular NDE technique for inspection of the defined defects is already set. All the laboratory experiments, and the mathematical and statistical analyses applied to the technique are to determine the POD but not to improve the POD of the inspection. Also, the characteristics of each NDE inspection are different. It is necessary to consider all the factors for the choice of a particular method for a specific type of material and defect. Conversely, POD must be remeasured for each new combination of material, defect, and inspection parameters.

Technically, a desirable inspection goal would be to choose an NDE procedure that has a detection limit slightly smaller than the critical inspection sizes. However, for an unknown defect, unless extensive experimental studies are performed to qualify a specific NDE method, the selection of the inspection technique for this defect can only be based on past experience of inspecting similar defect and material parameters.

III. ULTRASONIC C-SCAN IMAGING TECHNIQUE

Ultrasonic C-scan imaging is a well-established NDE technique for inspecting defects in various materials, including metals and composites. An ultrasonic C-scan system consists of three major components: ultrasonic instrumentation, a mechanical scanner, and a system controller. An ultrasonic pulser/receiver is used to excite and receive signals from a transducer. The transducer converts the electrical pulses into mechanical waves that propagate into the specimen. The mechanical scanner is an assembly of an X-Y scanning bridge, an immersion tank, and an associated transducer and sample fixture. A computer is generally used as the system controller for data acquisition, signal processing and image presentation.

For immersion C-scan tests, an immersion ultrasonic transducer traverses with a raster scanning pattern across the test specimen, which is positioned in a water tank. A stepless timing gate is imposed on the received ultrasonic RF signal from the specimen for comparison and analysis. The gated peak-detected ultrasonic signal amplitude is coordinated with each X-Y position scanned and used to generate the ultrasonic C-scan image: a false color, grayscale, or pseudo 3-D line drawing image. The block diagram of a typical ultrasonic C-scan imaging configuration is shown in Figure 4.
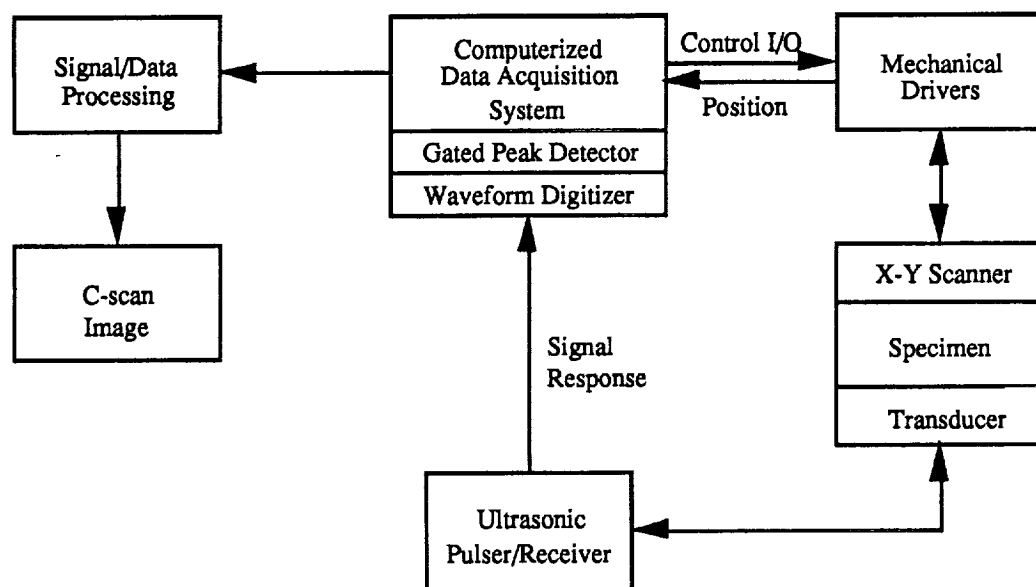

Figure 4. Block Diagram of an Ultrasonic C-scan Imaging System

The accuracy, sensitivity, and detectability of a system depend on the system components. The C-scan system used for our specific experiments is an off-the-shelf Physical Acoustics Corporation Ultrapac I ultrasonic imaging system. The system consists of a 30-MHz bandwidth Accu-Tron Inc. pulser/receiver, a 18.5" x 18.5" x 12" acrylic scanning tank, and a PC-XT compatible computer as the system controller. A data acquisition software package is provided with the system for instrument control, data acquisition, and image presentation. Except for the ultrasonic instrument, the mechanical scanner, the signal digitizer, and the time gate parameters can be set by the software. In the experiments, the time gate was positioned at the bottom of the tank. In this position, the pulse has travelled twice through the composite specimen. Redundant ultrasonic scans are done on each of the front and back sides of the four specimens. A total of 16 ultrasonic scans have been performed on four panels.

IV. COMPOSITE DELAMINATION SPECIMENS

To provide an adequate amount of data points for POD analyses, two sets of composite delamination panels were designed and fabricated. The FUSE project is a current GSFC in-house flight project and is the intended application for this POD study. This POD study effort will be used to ensure the integrity and quality assurance of FUSE composite structures. The design of the delamination specimens is thus based on the FUSE composite system. The test pieces were 16-ply thick, 10" by 10" square composite panels. The fiber and resin used in this composite system were T-300/934 with [+30/0/-30/90]2s lay-up order.

The delaminations were 16 circular Teflon inserts ranging from 1/16" to 1" in diameter in 1/16" increment for each composite specimen. The inserts were placed 2" from the edge and from each other. One set of delamination inserts was placed between the 8th and 9th ply on one composite panel. Another set of delamination inserts was alternately placed between the 4th and 5th, and the 12th and 13th plies on one panel. Let us refer delaminations between the 8th and 9th ply panels as Specimen **89** and delaminations between the 4th and 5th and between the 12th and 13th ply panels as Specimen **45**. There are two composite panels each for Specimen **89** and Specimen **45**. The sketch of these test delamination panels is shown in Figure 5.
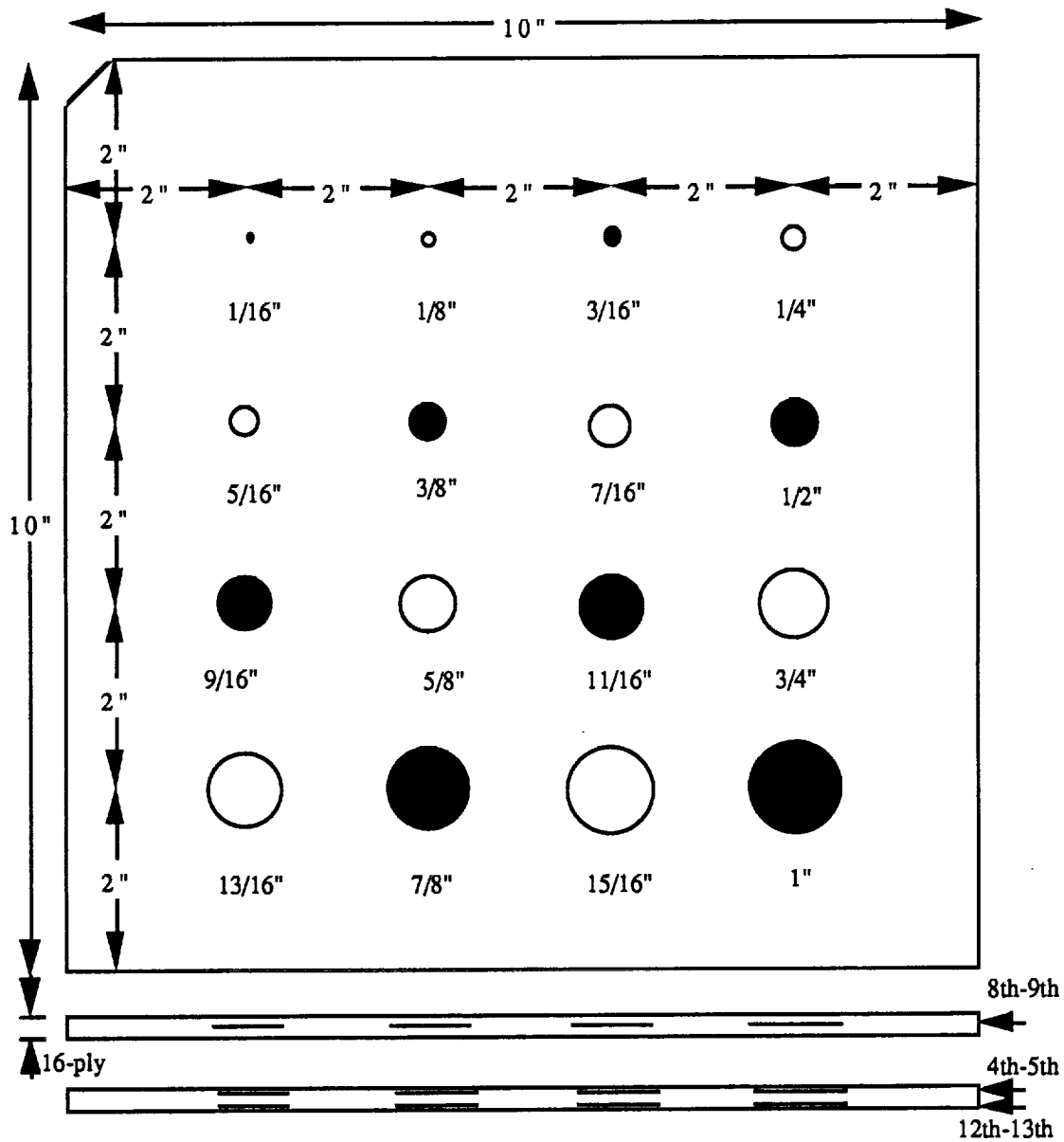
Figure 5. Composite Delamination Specimen Design

Since ultrasonic scans were performed on the front and back sides of each of the four specimens, there are a total of 8 data points for each size of delaminations for Specimen **89** and 8 data points for Specimen **45**. The two different depths of inserts in the Specimen **45** provide an additional variable in ultrasonic amplitude variations. The results of ultrasonic C-scans and POD analyses will be presented in the next section.

V. EXPERIMENTAL RESULTS AND POD ANALYSIS

(a) Ultrasonic C-scan

The generation of an ultrasonic C-scan image is based on the detected ultrasonic signal amplitude with respect to the transducer position on the specimen. With proper inversion algorithms, ultrasonic image can be correlated with the physical dimension of the object under investigation. However, the development of the exact inversion function depends on the complete solution of wave propagation and interaction with the object, and cannot easily be obtained. For a first order approximation, it is assumed that the size of the ultrasonic image is directly proportional to the physical size of the delamination.

All of the images obtained on the delamination in composites exhibit similar features. For the grayscale display of ultrasonic images, the grayscale represents descending ultrasonic amplitude received. The received ultrasonic signal will be strongest, i.e., white, when there is no obstruction of the wave path. The received ultrasonic signal will be the weakest, i.e., black, when the wave was deflected by the delamination. A typical ultrasonic C-scan image is shown in Figure 6. The specific image is for one of the two specimens with 1/16", 3/16", 3/8", 1/2", 9/16", 11/16", 7/8" and 1" diameter delaminations embeded between the 4th and 5th ply, and 1/8", 1/4", 5/16", 7/16", 5/8", 3/4" 13/16" and 15/16" diameter delaminations embeded between the 12th and 13th ply.

As can be easily seen visually, the standard ultrasonic C-scan technique can reliably detect delaminations down to 1/8" diameter in size or smaller. Other ultrasonic indications scattered in the image, outside the intended insert areas, were caused by surface wrinkles which were induced by imperfections of fabrication processes. The nonuniform structure of the surface reflects the ultrasonic energy away from the transducer and reduces the receiving ultrasonic amplitude. These ultrasonic indications correlate well with the actual panel surface geometry. Although qualitative statements can be made on the detectability of the delaminations and detection limits of the specific ultrasonic C-scan technique used, it is necessary to develop algorithms and perform statistical analyses on the detected ultrasonic images to obtain quantitative POD curves for the technique.
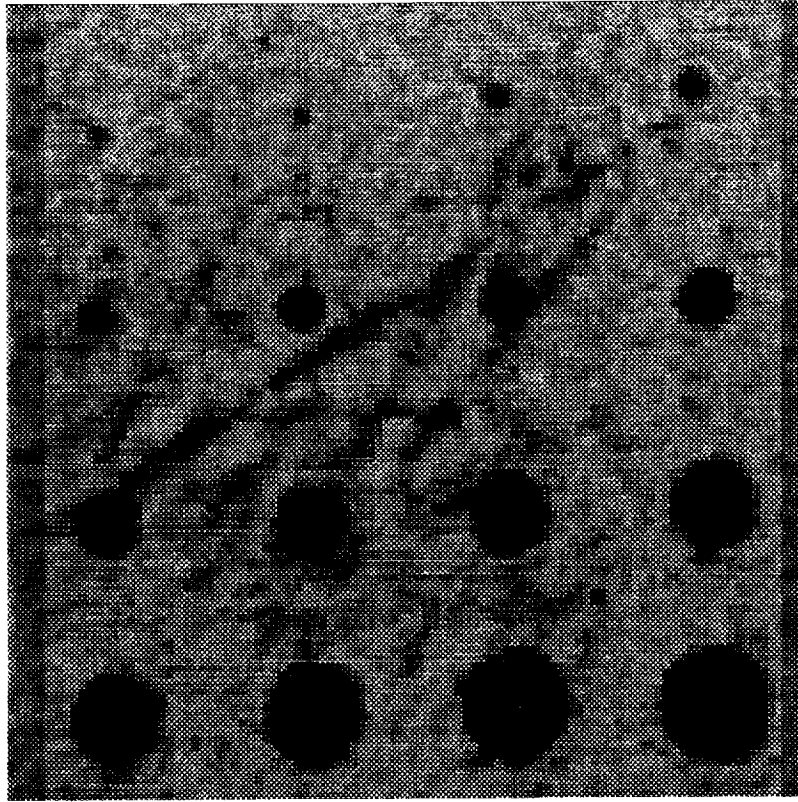
10

Figure 6. A typical Ultrasonic C-scan of Delaminations in Composites

(b) Determination of POD

The diameter of the delamination is selected as the defect parameter for this POD analysis. For a given measuring technique, the measured size (the diameter of the delamination image), $\hat{a}$ is a function of actual size, a, i.e. $\hat{a} = Rf(a)$. R is a random variable representing all the variabilities in the inspection process. If $f(a)$ is linear [$f(a) = a_0 + a_1 a$] and $R=1$, all data points (a, $\hat{a}$) should follow a straight line with the offset a_0 and slope a_1. A 45-degree straight line through (0,0) represents direct measurements of defects with the reference measuring technique. The measured defect sizes are normally plotted against actual defect sizes for assessment of $Rf(a)$. Plots for the $\hat{a}$ versus a for Specimen 89 and Specimen 45 are shown in Figure 7 and Figure 8, respectively.
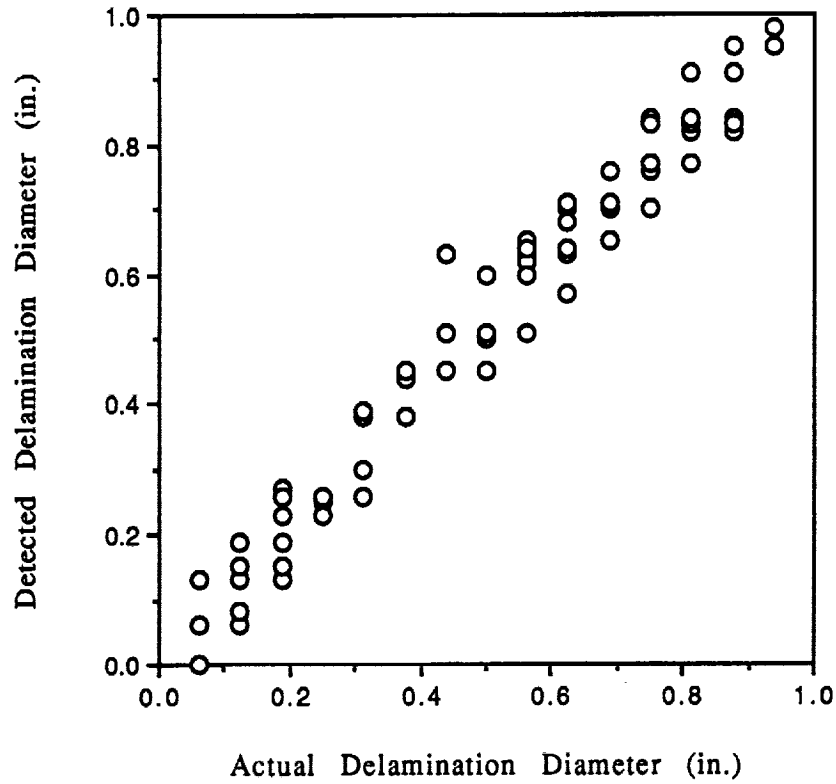
11

Figure 7. Measured Size $\hat{a}$ Versus Actual Size a for the Specimen **89**

In practice, a threshold value, denoted by $\bar{a}$, is often specified such that a specimen or structural component is rejected if the detected delamination size $\hat{a}$ is larger than the threshold value $\bar{a}$. The POD curve, denoted by $POD(\bar{a})$, is the probability that the detected delamination size is greater than the threshold value. With the mathematical analysis, $POD(\bar{a})$ can be expressed as

$$POD(\bar{a}) = \Phi \left[(\alpha + \beta \, ln \, a - ln \, \bar{a}) / s \right].$$

Where α and β are the parameters obtained from linear regression of the data, Φ is the standardized normal distribution function, and s is the standard deviation of the measurements. Parameters α, β, and s for Specimen **89** and Specimen **45** were calculated and listed in Table 1. With these parameters, a family of POD curves then can be calculated as a function of the threshold value $\bar{a}$.
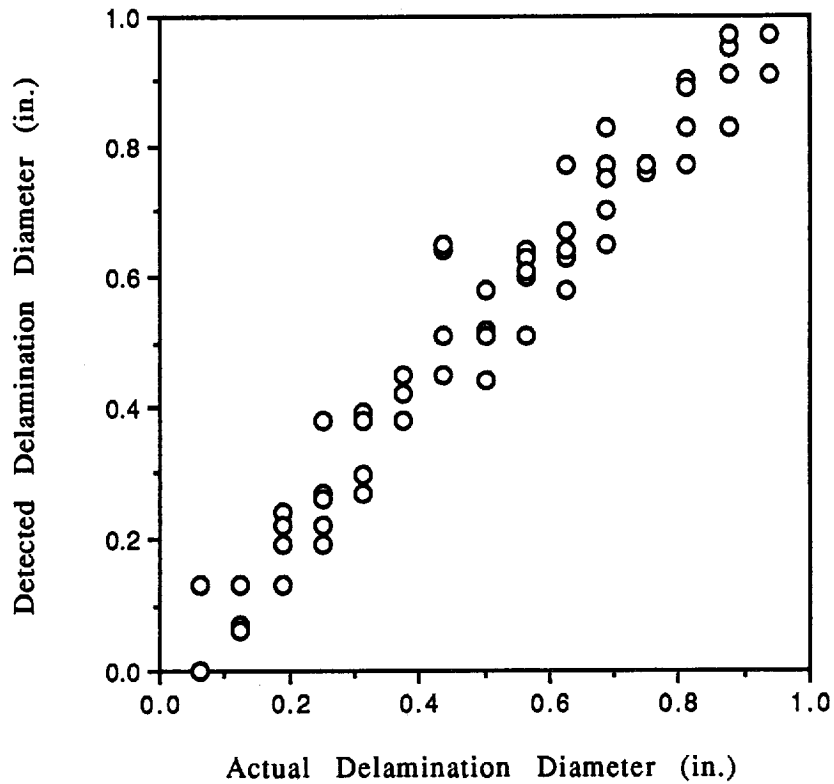
12

Figure 8. Measured Size $\hat{a}$ Versus Actual Size a for the Specimen **45**

Figure 9 is the plot of the 90/95 POD curve as a function of threshold level for Specimen **89**, and Figure 10 is the plot for Specimen **45**. As can be seen from the figures, ultrasonic C-scan imaging is very sensitive to delamination defects in composite materials. A 95% confidence level is established by using the 95 percentile of a chi-square distribution in the POD calculation. A 90% detectability and 95% confidence level (90/95) POD has been used extensively in the industry. A 90/95 POD is approximately 5/32" in diameter for Specimen **89** and 3/16" in diameter for Specimen **45**.

Table 1. Parameter Values for Delamination Data Sets

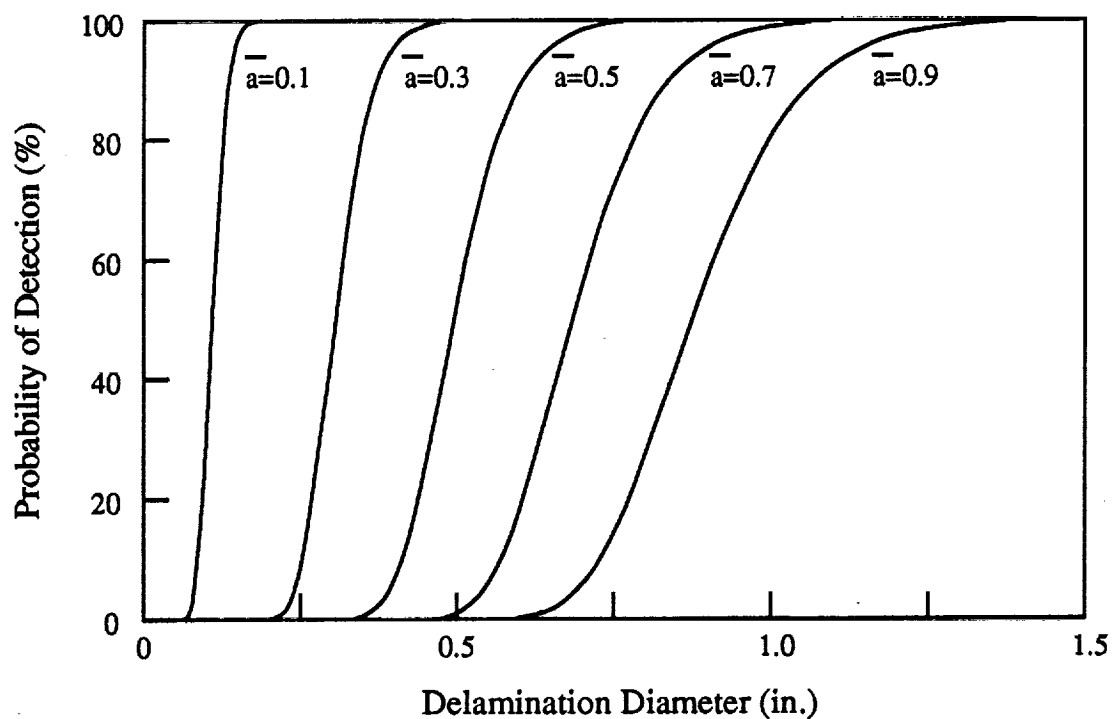| Delamination Location	α	β	s
Specimen **89**	0.067	1.03	0.146
Specimen **45**	0.122	1.16	0.179

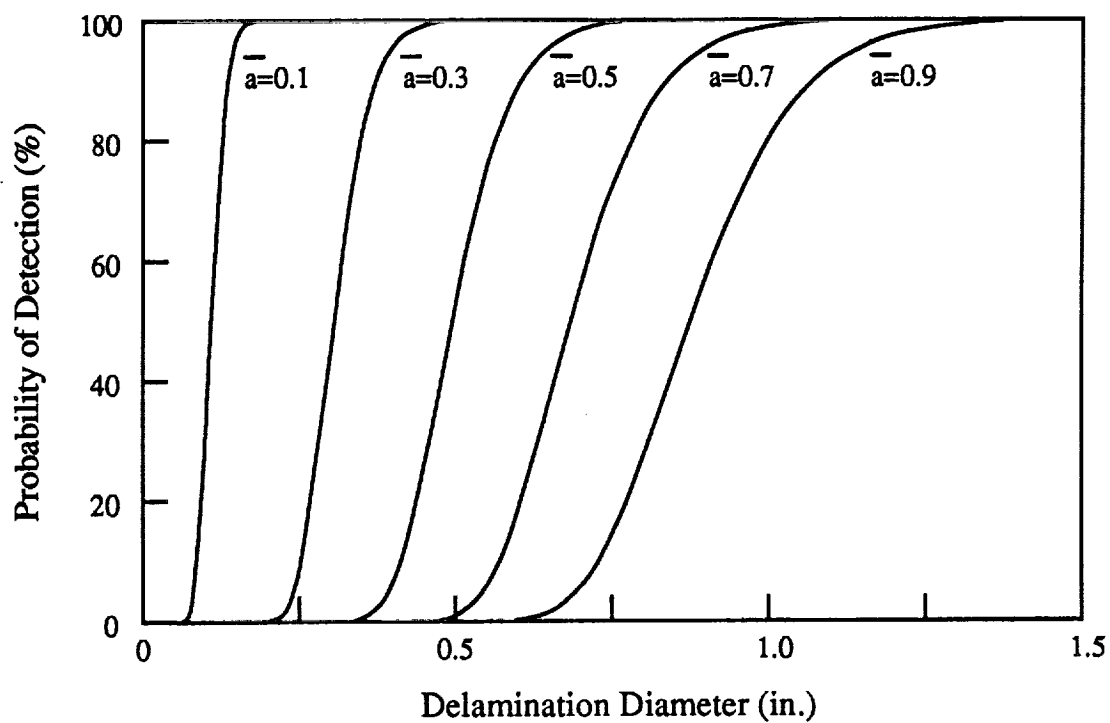Figure 9. POD Curves for the Specimen **89**

Figure 10. POD Curves for the Specimen **45**

14

VI. CONCLUSIONS

In conclusion, we have designed and fabricated composite delamination specimens, performed ultrasonic C-scan tests, and developed algorithms and analyzed POD. Based on the experimental results and POD analyses, a few remarks can be made concerning the ultrasonic C-scan imaging inspection of delaminations in composites:

(a) As can be seen from Figure 6, ultrasonic C-scan imaging technique is an excellent NDE technique for the detection of delaminations in composite panels.

(b) The bandwidth, the defect-size span of a given POD curve, is a measure of the detection uncertainty. The larger the bandwidth of the POD curve, the larger the Type I and Type II errors. All POD curves obtained have relatively small bandwidths, which imply that ultrasonic C-scan is a viable NDE technique.

(c) Based on ultrasonic C-scan images, the sensitivity of standard ultrasonic C-scan imaging for detecting delamination is estimated to be approximately 1/16" in diameter or smaller with 90/95 POD of 3/16" in diameter or larger.

(d) The sensitivity of the ultrasonic C-scan imaging technique can be improved with improved instrumentation such as higher operating frequency, focused transducer, and increased mechanical precision.

VII. REFERENCES

1. Yang, J. N., and R. C. Donath, "Improving NDE Capability Through Multiple Inspections with Application to Gas Turbine Engine," Air Force Wright Aeronautical Laboratories, Technical Report AFWAL-TR-82-4111, Wright-Patterson Air Force Base, August 1982.

2. Sturges, D. J., R. S. Gilmore, and P. W. Hovey, "Estimating Probability of Detection for Subsurface Ultrasonic Inspection," *Review of Progress in Quantitative NDE*, Vol. 5A, Plenum Press, New York, 1986, pp. 929-936.

3. McMaster, R. C., *Nondestructive Testing Handbook*, Ronald Press, New York, 1959.

4. Krautkramer, J., and H. Krautkramer, *Ultrasonic Testing of Materials*, Springer-Verlag, New York, 1983.

5. Kay, J., "Ultrasonic Image Synthesis - for NDT," in *Research Techniques in Nondestructive Testing*, Vol. 2, Academic Press, London , 1973, pp. 393-418.

6. Blake, R. A., "Quantitative Pseudocolor C-scan Evaluation and Enhancement," *Review of Progress in Quantitative NDE*, Vol. 3B, Plenum Press, New York, 1984, pp. 1051-1062.

7. Clark, G. A., D. M. Tilly, and W. D. Cook, "Ultrasonic Signal/Image Restoration for Quantitative NDE," *NDT International*, Vol. 19, June 1986, pp.169-176.

8. Frock, B. G., and R. W. Martin, "Digital Image Enhancement for Ultrasonic Imaging of Defects in Composite Materials," *Materials Evaluation*, Vol. 47, April 1989, pp. 442-447.

9. Blake, R. A., "Image Processing of Composite Materials Using Ultrasonic Nondestructive Evaluation Data," *Non-destructive Testing of Fibre-reinforced Plastics Composites*, Vol. 2, Elsevier Applied Science, London and New York, 1990, pp. 161-200.

REPORT DOCUMENTATION PAGE

Public reporting burden for this collection of information is estimated to average 1 hour per response, including the time for reviewing instructions, searching existing data sources, gathering and maintaining the data needed, and completing and reviewing the collection of information. Send comments regarding this burden estimate or any other aspect of this collection of information, including suggestions for reducing this burden, to Washington Headquarters Services, Directorate for Information Operations and Reports, 1215 Jefferson Davis Highway, Suite 1204, Arlington, VA 22202-4302, and to the Office of Management and Budget, Paperwork Reduction Project (0704-0188), Washington, DC 20503.

1. AGENCY USE ONLY (Leave blank)	2. REPORT DATE December 1991	3. REPORT TYPE AND DATES COVERED Technical Memorandum

4. TITLE AND SUBTITLE

Assessment of Probability of Detection of Delaminations in Fiber-Reinforced Composites

5. FUNDING NUMBERS

6. AUTHOR(S)

E. J. Chern, H. P. Chu and J. N. Yang

7. PERFORMING ORGANIZATION NAME(S) AND ADDRESS(ES)

NASA Goddard Space Flight Center
Greenbelt, Maryland 20771

8. PERFORMING ORGANIZATION REPORT NUMBER

92B00022

9. SPONSORING/MONITORING AGENCY NAME(S) AND ADDRESS(ES)

National Aeronautics and Space Adminstration
Washington, D.C. 20546-0001

10. SPONSORING/MONITORING AGENCY REPORT NUMBER

NASA TM-104553

11. SUPPLEMENTARY NOTES

E. J. Chern and H. P. Chu: NASA Goddard Space Flight Center, Greenbelt, Maryland
J. N. Yang: University of California, Irvine, California

12a. DISTRIBUTION/AVAILABILITY STATEMENT

Unclassified - Unlimited

Subject Category 71

12b. DISTRIBUTION CODE

13. ABSTRACT (Maximum 200 words)

Delamination is one of the critical defects in composite materials and structures. Ultrasonic C-scan imaging technique which maps out the acoustic impedance mismatched areas with respect to the sample coordinates, is particularly well suited for detecting and characterizing delaminations in composites. To properly interpret the results, it is necessary to correlate the indications with the detection limits and probability of detection (POD) of the ultrasonic C-scan imaging technique. The baseline information on the assessment of POD of delaminations in composite materials and structures is very beneficial to the evaluation of spacecraft materials. In this study, we review the principle of POD, describe the laboratory set-up and procedure, and present the experimental results as well as assessment of POD of delaminations in fiber-reinforced composite panels using ultrasonic C-scan techniques.

14. SUBJECT TERMS

Ultrasonic C-scan Imaging
Delaminations in Composites
Probability of Detection

15. NUMBER OF PAGES

20

16. PRICE CODE

17. SECURITY CLASSIFICATION OF REPORT Unclassified	18. SECURITY CLASSIFICATION OF THIS PAGE Unclassified	19. SECURITY CLASSIFICATION OF ABSTRACT Unclassified	20. LIMITATION OF ABSTRACT

NSN 7540-01-280-5500